

# Initial state dependence of the breakup of weakly bound carbon isotopes

Angela Bonaccorso\*

*Istituto Nazionale di Fisica Nucleare, Sezione di Pisa, I-56100 Pisa, Italy*

(Received 22 April 1999; published 27 September 1999)

The one-neutron nuclear breakup from the carbon isotopes  $^{19}\text{C}$  and  $^{17}\text{C}$ , is calculated as an example of application of the theory of transfer to the continuum reactions in the formulation which includes spin coupling. The effect of the energy sharing between the parallel and transverse neutron momentum distributions is taken into account, thus resulting in a theory which is more general than sudden eikonal approaches. Both effects are necessary to understand properly the breakup from not too weakly bound  $l_i > 1$  orbitals. Breakup which leads the core into an excited state below particle threshold is also considered. The core-target interaction is treated in the smooth cutoff approximation. By comparing to presently available experimental data we show how to make some hypothesis on the quantum numbers and occupancy of the neutron initial state. Possible ambiguities in the interpretation of inclusive cross sections are discussed. [S0556-2813(99)05910-5]

PACS number(s): 25.70.Hi, 21.10.Gv, 25.60.Gc, 25.70.Mn

## I. INTRODUCTION

In last ten years since the advent of radioactive beams (RIB's) [1] a new phenomenon called "nuclear halo" [2] has appeared in nuclear physics. There is a halo on a nucleus as  $^{11}\text{Be}$  when the last neutron or the last couple of neutrons, as in  $^{11}\text{Li}$ , are very weakly bound and in a single particle state of low angular momentum ( $s$  or  $p$ ). Then the single particle wave function has a long tail which extends mostly outside the potential well. Because of these characteristics the reactions initiated by such nuclei give large reaction cross sections and neutron breakup cross sections. Also the ejectile parallel momentum distributions following breakup are very narrow, typically 40–45 MeV/ $c$ . There are also some candidates for a proton halo, such as  $^8\text{B}$  [3–5]. But because of the Coulomb barrier which keeps the wave function localized at the interior, there is still not clear experimental evidence for this phenomenon.

More recently another radioactive nucleus  $^{19}\text{C}$  has been produced but the presence of a halo is still under discussion. There is a number of experimental and theoretical studies of this nucleus whose results point to a complex picture of its structure. Because of the presence of  $d$  components in the neutron wave function the reaction mechanism is rather more complicated than for a simple  $s$ -halo state and therefore it is more important to be able to disentangle structure effects from effects due to the reaction dynamics.

Two sets of experiments from MSU at  $E_{inc} = 77$  and  $88A$  MeV have given rather large nuclear and Coulomb breakup cross sections and narrow parallel momentum distributions [6,7]. Consistent results were obtained from a RIKEN experiment [8] of Coulomb breakup. A distribution similar in shape to the MSU distribution but wider has been measured at GSI [9] in a nuclear breakup experiment at  $910A$  MeV. On the other hand a GANIL experiment based on the core-breakup reaction mechanism at  $E_{inc} = 30A$  MeV gave a narrow neutron angular distribution [10]. The first measurement of the interaction cross sections

at GANIL [11] did not seem to support the presence of a halo, while very recently rather large interaction cross sections have been measured at RIKEN [12]. One of the following sections is devoted to a brief review of the structure calculations so far published.

In this paper we study the nuclear breakup of  $^{19}\text{C}$  and  $^{17}\text{C}$  using the theory of transfer to the continuum [13–20]. In [14,15] we have shown that it is well adapted to describe the halo breakup and we found that our calculations were in good agreement with experimental breakup cross sections [21] and the parallel momentum distribution widths [22]. The transfer to the continuum formalism can deal with any initial binding energy and angular momentum state. It is valid in the intermediate energy domain ( $E_{inc} = 10 - 100A$  MeV) since it treats the relative nucleus-nucleus scattering semiclassically. The neutron transition amplitude is, however, treated quantum mechanically. Therefore the method is of intermediate complexity between the DWBA approach introduced in [23] and simplified in [24] and the eikonal-type of approaches used by several authors [25–34] to treat the special case of halo breakup. Our approach contains several improvements with respect to previous breakup theories in particular insofar as the calculations of the neutron and ejectile parallel momentum distributions are concerned. One is the introduction of spin coupling factors discussed below. Also we treat consistently the absorption and elastic breakup of the neutron on the target via an unitary optical model  $S$ -matrix. Since we do not make the sudden hypothesis our formalism is more general than some eikonal models while reducing to an eikonal form in the limit of zero binding energy, as was shown in [15]. Furthermore we introduce and study the effect of a smooth cutoff approximation in the treatment of the ion-ion scattering.

## II. REACTION MODEL

We do not give details of the theory here but use its main final formulas. The theory of transfer to the continuum treats on equal footing the elastic breakup of the neutron and its absorption from the elastic channel by the target via an optical model final state wave function which depends on an

\*Electronic address: ANGELA.BONACCORSO@PI.INFN.IT

unitary neutron-target  $S$ -matrix.

The neutron breakup probability distribution in the projectile reference frame is

$$\frac{dP}{dk_1} \approx \frac{1}{2} \sum_{j_f} (|1 - \langle S_{j_f} \rangle|^2 + 1 - |\langle S_{j_f} \rangle|^2) (2j_f + 1) \times (1 + R) B_{l_f, l_i}. \quad (2.1)$$

It is obtained from a quantum mechanical transition amplitude [16] which represents the overlap between the neutron momentum distributions in the initial and final state when the projectile core is at a distance  $d$  from the target. The projectile-target relative motion is treated semiclassically by using a trajectory of the center of the projectile relative to the center of the target  $\mathbf{s}(t) = \mathbf{d} + \mathbf{v}t$  with constant velocity  $\mathbf{v}$  in the  $z$  direction and impact parameter  $\mathbf{d}$  in the  $xy$  plane.  $\langle S_{j_f} \rangle$  is the energy averaged and spin dependent optical model  $S$ -matrix which describes the neutron target interaction. Then the first term in Eq. (2.1), proportional to  $|1 - \langle S_{j_f} \rangle|^2$  gives the neutron elastic breakup or diffraction, while the second term proportional to  $1 - |\langle S_{j_f} \rangle|^2$  gives the neutron absorption (or stripping) by the target.  $B_{l_f, l_i}$  is an elementary transfer probability which depends on the energies  $\varepsilon_i$  and  $\varepsilon_f$ , momenta  $\gamma_i$  and  $k_f$ , and angular momenta  $l_i$  and  $l_f$  of the initial and final neutron single particle states, respectively, and on the incident energy per particle,  $m v^2/2$  at the distance of closest approach  $d$ :

$$B_{l_f, l_i} = \left[ \frac{\hbar}{m v} \right] \frac{1}{k_f} |C_i|^2 \frac{e^{-2\eta d}}{2\eta d} M_{l_f, l_i}, \quad (2.2)$$

where  $M_{l_f, l_i} = 1/(\sqrt{\pi}) \int_0^\infty dx e^{-x^2} P_{l_i}(X_i + B_i x^2) P_{l_f}(X_f + B_f x^2)$  and  $X_i = 1 + 2(k_1/\gamma_i)^2$ ,  $X_f = 2(k_2/k_f)^2 - 1$ ,  $B_i = 2\eta/d \gamma_i$ , and  $B_f = 2\eta/d k_f$ .  $k_1 = (\varepsilon_f - \varepsilon_i - \frac{1}{2} m v^2)/(\hbar v)$  and  $k_2 = (\varepsilon_f - \varepsilon_i + \frac{1}{2} m v^2)/(\hbar v)$  are the  $z$  components of the neutron momentum in the initial and final state, respectively.  $\eta^2 = k_1^2 + \gamma_i^2 = k_2^2 - k_f^2$  is the magnitude of the transverse component  $k_\perp = i\hbar \eta$  of the neutron momentum in the initial and final state.  $k_\perp$  is conserved during the breakup process and it is purely imaginary because the neutron which in the initial state has negative energy [35] is emitted through a potential barrier. Because of this it holds also  $k_2 > k_f$ . It is straightforward to see from the definitions of these kinematical variables that they satisfy the neutron energy and momentum conservation. The effect of their variation on the reaction mechanism will be discussed in the following.

In Eq. (2.1)  $R$  is a dynamical factor which depends on several variables of the transfer reaction, namely the  $Q$  value and the incident energy. In the case of nucleon transfer for a given channel specified by  $(l_f, l_i)$  this factor weighs the selectivity with respect to the four possible transfers:

$$j_i = l_i \pm \frac{1}{2} \rightarrow j_f = l_f \pm \frac{1}{2},$$

TABLE I. Coefficients  $D_{j_f, j_i}$ .

$j_i$	$l_i - \frac{1}{2}$	$l_i + \frac{1}{2}$
$j_f$		
$l_f - \frac{1}{2}$	$\frac{1}{l_i l_f}$	$\frac{-1}{l_f(l_i + 1)}$
$l_f + \frac{1}{2}$	$\frac{-1}{l_i(l_f + 1)}$	$\frac{1}{(l_i + 1)(l_f + 1)}$

$$j_i = l_i \pm \frac{1}{2} \rightarrow j_f = l_f \mp \frac{1}{2}.$$

The explicit form of  $R$  is  $R = D_{j_f, j_i} F(\varepsilon_f)$  where  $D_{j_f, j_i}$  is given in Table I and

$$F(\varepsilon_f) = -F(k_1, l_i, \eta, \gamma_i) F(k_2, l_f, \eta, k_f)$$

where

$$F(k, l, \eta, \gamma) = \frac{2k\eta}{\gamma^2 P_l(X)} \frac{dP_l(X)}{dX}.$$

From Table I we see that  $D_{j_f, j_i}$  has a negative sign for the spin-flip transitions  $j_i = l_i \pm \frac{1}{2} \rightarrow j_f = l_f \mp \frac{1}{2}$  and a positive sign for the opposite situation  $j_i = l_i \pm \frac{1}{2} \rightarrow j_f = l_f \pm \frac{1}{2}$ .

Equation (2.1) is more general than the breakup probability discussed in [15] because it includes spin. We use it in this paper to check the sensitivity of the breakup cross sections and parallel momentum distribution widths to changes in the initial spin of the neutron. For example in the case of a  $d$  state both  $1d_{3/2}$  or  $1d_{5/2}$  orbits could be occupied. The derivation of the above equations has been given by Hashim and Brink [36] in the case of bound-state to bound-state transfer and was extended by us [18] to the final continuum case.

Finally the cross section [14,15] is given by an integration over the core-target impact parameter

$$\frac{d\sigma_{1n}}{dk_1} = C^2 S \int_0^\infty d\mathbf{d} \frac{dP(d)}{dk_1} P_{el}(d). \quad (2.3)$$

The total breakup cross section is obtained by integrating over  $dk_1$ .  $C^2 S$  is the spectroscopic factor of the neutron single particle wave function in the initial state. The factor  $P_{el}(d) = |S_{el}|^2$  is the core survival probability in the elastic channel written in terms of the  $S$ -matrix for the core-target scattering. Since the conditions for the semiclassical approximation to the relative ion-ion scattering apply for the reactions discussed in this paper, we use the following parametrized form which has already been discussed in [37]:

$$P_{el}(d) = \exp(-\ln 2 \exp[(R_s - d)/a]). \quad (2.4)$$

When the breakup probability is not too peaked as a function of  $d$ , the above form gives a better approximation to the cross section than the strong absorption limit used in [15]. This happens if the decay parameter  $\eta$  of the breakup prob-

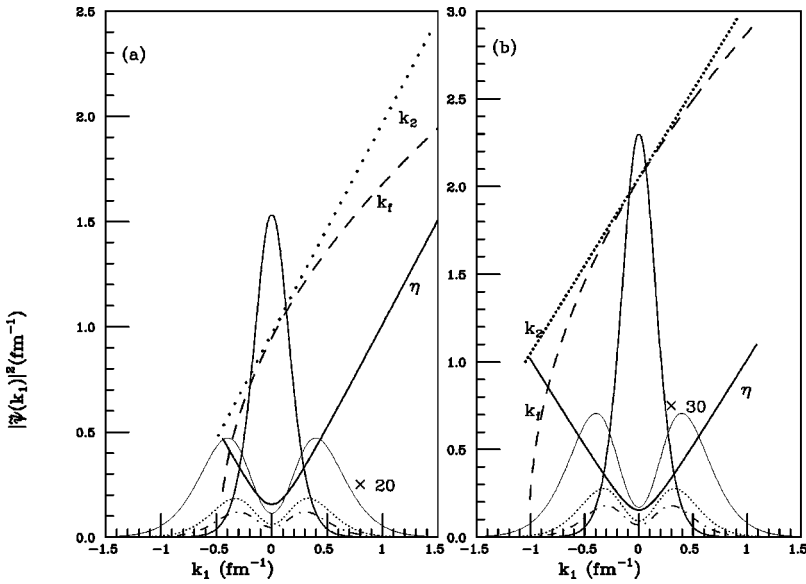


FIG. 1. Initial state momentum distributions, Eq. (2.5), as a function of  $k_1$ , the neutron parallel momentum component in the initial state. For an  $s$  state with  $\rho=6.5$  fm, full curve peaked at  $k_1=0$ . For a  $d$  state: dot-dashed, dotted, and thin solid curves are at  $\rho=6.5$  fm, 6 fm, 5 fm, respectively. The dotted line is  $k_2$ , the neutron parallel momentum component in the final state; the dashed line is  $k_f$ , the neutron total final momentum and the solid line is  $\eta$ , the neutron transverse momentum component. (a)  $E_{inc}=20A$  MeV, (b)  $E_{inc}=88A$  MeV.

ability is not very small, corresponding to a not too small initial binding, and when the initial angular momentum  $l_i$  is different from zero. The strong absorption radius  $R_s$  [14,15,37] is defined by  $P_{el}=1/2$  and  $a$  is a diffuseness parameter whose values will be discussed in the following.

Equation (2.3) gives the final neutron parallel momentum distribution which is related by momentum conservation to the measured ejectile momentum distribution [15].

#### A. Relation to sudden approaches

We discuss now in more detail the relation between our model and sudden eikonal approaches. In this paper our main interest is to clarify the effect of a time dependent approach on the shapes and widths of the neutron and of the ejectile parallel momentum distributions following one-neutron breakup. The range of validity of the sudden approximation in such a context has recently been discussed in [33]. The discussion and the results presented there suggest that it is best suited for incident energies larger than 150A MeV, for very weak neutron binding and low initial angular momentum states ( $l_i=0,1$ ). Under the original Glauber terminology the same approximation is often called adiabatic because the internal relative motion of the particles is considered slow with respect to the relative motion of the colliding nuclei. In this sense it has been used in [28,38,39] where it was found appropriate to reproduce several other measured quantities such as the ejectile angular distributions following neutron breakup and the absolute cross sections at relativistic energies.

Under the sudden (or adiabatic) hypothesis the parallel momentum distribution of the neutron in the projectile is frozen during the reaction and its shape should be reflected by the final measured distribution. The available neutron final energy is all converted into parallel momentum. Interference effects with the transverse distribution are in this way neglected. The sudden hypothesis means also that the whole momentum distribution in the initial state is sampled during the reaction, while in our approach the kinematical condi-

tions, expressed in the definition of  $k_1$  and  $k_2$ , make a selection on the part of the initial distribution which can be sampled by the reaction. Also, in the present approach in order to realize the best energy matching conditions for each possible final energy  $\varepsilon_f$  of the neutron, the reaction mechanism shares the total momentum  $k_f$  between the transverse momentum component  $\eta$  and the parallel component  $k_2$ , thus allowing the interference [cf. also Eq. (3) of [14]] between the two corresponding distributions. The factor  $M_{l_i}$  in Eq. (2.2) shows explicitly how the interference comes about. As a consequence the measured parallel momentum distribution might look deformed as compared to the original parallel momentum distribution of the neutron in the initial state of the projectile.

In order to clarify the importance of the energy sharing between the parallel and transverse components of the neutron final momentum, we show in Figs. 1(a) and 1(b), corresponding to an incident energy of 20A MeV and 88A MeV, respectively, the following kinematical variables as functions of  $k_1$  the neutron initial momentum with respect to the projectile:  $k_2$ , the neutron final parallel momentum component with respect to the target, by the dotted line;  $k_f$ , the magnitude of the total neutron momentum corresponding to each neutron final continuum energy  $\varepsilon_f$ , by the dashed line;  $\eta$  the neutron transverse momentum component, by the solid line. The minimum values of  $k_1$  correspond to  $\varepsilon_f=0$  MeV. Clearly values of all parameters corresponding to values of  $\varepsilon_f<0$  are not accessible by breakup reactions but they would rather correspond to transfer to a final bound state. In both figures there is a region corresponding to very small values of  $\eta$  in which  $k_2 \approx k_f$ . This is the region of validity of the sudden eikonal approximation. In fact in such conditions since the transverse component of the neutron momentum  $\eta$  is very small, the total momentum  $k_f$  is all converted into parallel momentum  $k_2$ . In [14] we showed indeed that the condition  $k_2 \approx k_f$  was necessary to obtain the eikonal form of the breakup amplitude. In the same figures we show the initial  $s$  and  $d$  distributions of the parallel neutron momentum as a function of  $k_1$ . They are obtained from

$$\begin{aligned}
|\tilde{\psi}_i(\rho, k_1)|^2 &= \sum_{m_i} |2C_i Y_{l_i, m_i}(\hat{k}_1) K_{m_i}(\eta\rho)|^2 \\
&\approx |C_i|^2 \frac{e^{-2\eta\rho}}{2\eta\rho} P_{l_i}(X_i), \quad (2.5)
\end{aligned}$$

which is the one-dimensional Fourier transform of the asymptotic part of the initial state wave function [15,35] used to get Eq. (2.1) [15].  $C_i$  are the initial wave function asymptotic normalization constants given in Table II.  $K_{m_i}$  are modified Bessel functions of the second kind. The Legendre polynomial  $P_{l_i}$  and its argument  $X_i$  have already been defined. The initial distribution depends on  $\rho$ , which is the neutron distance from the projectile center in the  $x$ - $y$  plane perpendicular to the relative velocity axis between the two ions which is chosen as the  $z$  direction. The thick solid ( $s$  distribution) and dot-dashed ( $d$  distribution) lines are obtained at  $\rho=6.5$  fm, which is close to the strong absorption radius value in the case of the  $^{19}\text{C}+^9\text{Be}$  reaction. In heavy-ion collisions the strong absorption radius is energy dependent and it decreases increasing the beam energy. For this reason we show also by the dotted and thin-solid lines the  $d$  distributions calculated at  $\rho=6$  and 5 fm, respectively. In this case the distributions are wider. This is one of the origins for a possible widening of the widths when the incident energy increases. The initial distributions also get wider by increasing the absolute value of the initial binding. Therefore the eikonal approximation is best justified in a range of  $k_1 \approx 0$  values and for initial distributions, such as the  $l_i=0$  one, concentrated in such a region. Figure 1(b) shows that such a range increases by increasing the incident energy. On the other hand Fig. 1(a) shows that at incident energies around 20A MeV an important part of the initial neutron momentum distribution corresponding to  $k_1$  values from  $-\infty$  to about  $-0.5 \text{ fm}^{-1}$  would not be kinematically allowed. Thus using the frozen limit would give too wide momentum distributions and too large breakup cross sections. This is consistent with the recent discussion in [34].

Figures 2(a) and 2(b) show the neutron parallel distribution after breakup from a  $d$  orbital with  $\varepsilon_i = -1.86$  MeV, in the projectile reference frame, for the two initial beam energies used in Figs. 1(a) and 1(b). Such distributions are calculated in the spin-independent approach. The solid line is the total breakup distribution obtained from the sum of the elastic breakup (dotted line) and absorption (dot-dashed line). In both cases the distributions are deformed with respect to the initial symmetrical one. In particular it is interesting to see in the case of  $E_{inc}=20$  MeV that elastic breakup dominates at small initial  $k_1$  while absorption of the neutron on the target is responsible for the long tail at large  $k_1$  in both cases. The total widths are very different. At  $E_{inc}=20$  MeV we get  $\hbar\Delta k_1=142$  MeV/ $c$  while at  $E_{inc}=88A$  MeV we get  $\hbar\Delta k_1=177$  MeV/ $c$ , also the deformation effects are less evident in the latter case. The strong asymmetry of the distributions can therefore be seen as a consequence of the behavior of  $\eta$  as a function of  $k_1$  shown in Fig. 1(a). This shows that the beam energy dependence of the widths is due in part to the different range of kinematically accessible variables  $k_1$ ,  $k_2$ , and  $\eta$ .

## B. Spin effects

To understand the sensitivity of the calculated spectra to the initial state spin we show in Fig. 3(a) the neutron parallel distribution after breakup from a  $d_{3/2}$  orbital at  $E_{inc}=88A$  MeV. In Fig. 3(b) we show the distribution after breakup from an initial  $d_{5/2}$  instead. In both figures the dotted line is the elastic breakup, from the first term of Eq. (2.1), the dashed line is the absorption (or stripping) from the second term of Eq. (2.1). The solid line is the sum of the two giving the inclusive spectrum. It is interesting to notice that the absorption spectrum is very similar in the two cases. This is due to the fact that at high energies the absorption depends mainly on the imaginary part of the neutron-target optical potential while it is rather insensitive to the spin-orbit real potential. The elastic breakup gives instead different spectra depending on the initial spin. As a consequence the neutron transverse distributions should also be different, and an experimental measure of them would help determine the total angular momentum of the initial state, as has been already done in [41]. Clearly, interference and spin effects will show up best in the data when just one initial angular momentum state is responsible for the measured breakup.

In both cases the initial symmetrical  $d$  distribution which has two peaks in Fig. 1(b) has undergone a distortion because of the reaction mechanism. The distortion is different for the two initial states  $j_i=l_i \pm \frac{1}{2}$ . This is a quantum mechanical effect, due to the dependence of the spin coupling factors on the reaction  $Q$  value and then to the final neutron energy. It does not have a simple classical interpretation but we can explain the origin of it in our formalism. In the sum over final angular momenta  $j_f$  in Eq. (2.1), all states with  $j_f=l_f+\frac{1}{2}$  are favorite with respect to the  $j_f=l_f-\frac{1}{2}$  for each  $l_f$  because the neutron-target spin-orbit interaction is larger the larger the angular momentum, and then the elastic scattering probability proportional to  $|1-\langle S_{j_f} \rangle|^2$  is largest. For the same reason the neutron leaves the projectile more easily if it is in a  $j_i=l_i-\frac{1}{2}$  state corresponding to a smaller neutron-core spin-orbit interaction. On the other hand the dependence of the spin coupling factor  $F_{l \rightarrow j}=2j+1/(2)(1+R)$  in Eq. (2.1) on the neutron final energy is such that the  $j_f=l_f+\frac{1}{2}$  states are more favorite at high neutron energy in a spin flip transition  $j_i=l_i-\frac{1}{2} \rightarrow j_f=l_f+\frac{1}{2}$  while they are more favorite at lower neutron final energy in a no-spin-flip transition such as  $j_i=l_i+\frac{1}{2} \rightarrow j_f=l_f+\frac{1}{2}$ . The behavior of  $F_{l \rightarrow j}$  as

TABLE II. Initial state parameters.

Projectile	$ \varepsilon_i $ (MeV)	$C_i$ ( $\text{fm}^{-1/2}$ )		
$^{17}\text{C}$	0.73	1.06	0.110	0.105
	2.50	2.60	0.500	0.470
$^{19}\text{C}$	0.24	0.65	0.038	0.035
	0.50	0.89	0.078	0.074
	1.86	1.94	0.336	0.314
	2.12	—	0.390	—
Initial state		$2s_{1/2}$	$1d_{5/2}$	$1d_{3/2}$

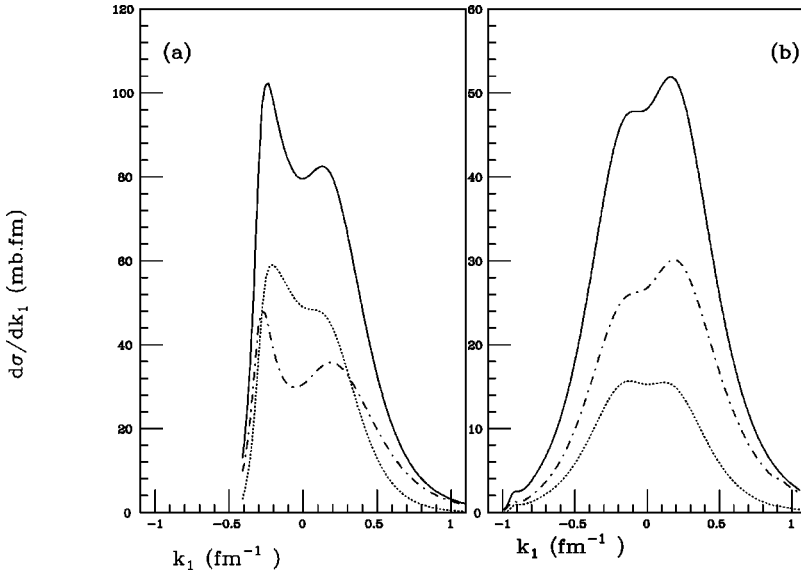


FIG. 2. The neutron final parallel momentum distribution in the projectile reference frame for a  $d$  state at  $d=6.5$  fm and  $\varepsilon_i=-1.86$  MeV in  $^{19}\text{C}$ . (a)  $E_{inc}=20A$  MeV, (b)  $E_{inc}=88A$  MeV.

a function of  $k_1$  is shown in the two small figures on top of Figs. 3(a) and 3(b) in the case of  $l_f=4$ . Notice that at any  $k_1$  the  $F_{l \rightarrow j}$  coefficients satisfy  $F_{l \rightarrow j_+} + F_{l \rightarrow j_-} = 2l_f + 1$ . Such spin coupling effects, depending on the reaction  $Q$  value, are a generalization of those known in transfer between bound states and discussed among others in [36,37,42]

### III. STRUCTURE OF HEAVY CARBON ISOTOPES

The carbon isotopes with mass number  $A=17-19$  belong to the category of  $2s-1d$  shell nuclei whose structure is only partially understood at present. In a simple central plus spin-orbit potential of independent particles the last neutron in  $^{19}\text{C}$  should be in a  $1d_{5/2}$  state but more accurate shell model calculations [43] and relativistic mean-field [44] find that the last occupied orbit is a  $2s_{1/2}$  state with spectroscopic factor 0.58 giving a  $1/2^+$  ground state. Coupled channel cal-

culations give a series of possibilities in which the wave function is a  $s$  or  $d$  state coupled to the  $0^+$  or  $2^+$  states of the core [45,46]. In [9] dynamical core polarization calculations are reported which give a  $1/2^+$  ground state with 40% occupancy for  $^{18}\text{C}(0^+) \otimes 2s_{1/2}$ , the rest of the wave function is given by the  $^{18}\text{C}(2^+) \otimes 1d_{5/2}$  configuration. In [6,7,9,46]  $^{17}\text{C}$  was also studied. The ground state of this nucleus could be  $0^+ \otimes 1d_{3/2}$  [7,9], but the shell model calculation quoted in [7] suggests also the possibility

$$0.16 \times (2^+ \otimes 2s_{1/2}) + 1.58 \times (2^+ \otimes 1d_{5/2}).$$

In all cases if the last neutron is in a pure single particle state, the possibilities  $l_i=0$  or  $l_i=2$  and  $d_{3/2}$  or  $d_{5/2}$  should be easily distinguished by comparing theoretical calculations to the experimental data for one neutron breakup. However as we have mentioned above both states could be only par-

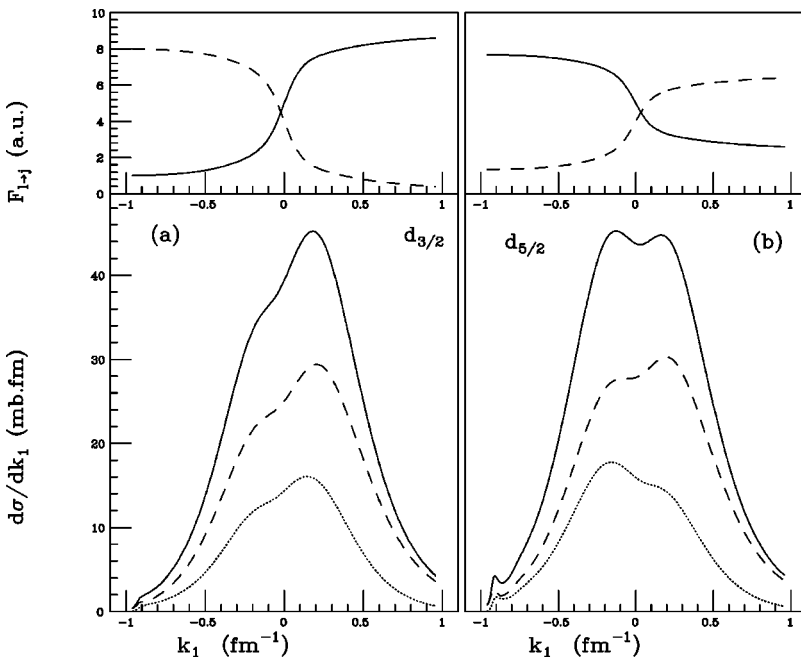


FIG. 3. The neutron final parallel distribution in the projectile reference frame for a  $d$  state at  $E_{inc}=88A$  MeV. (a)  $d_{3/2}$ ,  $j_i=l_i-1/2$ ; (b)  $d_{5/2}$ ,  $j_i=l_i+1/2$ . Top figures give the corresponding spin coupling coefficients  $F_{l \rightarrow j}$  for  $l_f=4$ . Solid line  $j_i \rightarrow j_f=l_f+1/2$ , dashed line  $j_i \rightarrow j_f=l_f-1/2$ .

tially occupied and coupled to ground state or to core excited states. Inclusive experimental data can contain contributions from several core excited states which can eventually be discriminated by a  $\gamma$ -ray experiment like the one described in [47]. Such a situation is quite common in heavy-ion induced reactions. For example, in the case of a “normal” nucleus like  $^{40}\text{Ar}$  we showed in [20] that there are several possible initial states corresponding to core excited states, all contributing to the experimental spectrum. In particular we showed that initial states of different angular momenta lead to different shapes for the ejectile inclusive spectra and that the experimental spectrum was indeed dominated by the contribution from a  $1d_{3/2}$  coupled to a core excited state. This was due to the spin coupling effects.

#### IV. RESULTS

As an application of our theory and in the attempt to shed some light on the  $^{19}\text{C}$  and nearby isotope structure we have made some sample calculations and a preliminary comparison with presently available experimental data. The following quantities have been investigated. (i) One neutron nuclear breakup cross sections from  $^{19}\text{C}$  on  $^9\text{Be}$ ,  $^{12}\text{C}$ , and  $^{208}\text{Pb}$  targets and  $^{17}\text{C}$  on  $^9\text{Be}$ . (ii) neutron parallel momentum distributions for the same reactions.

The initial state parameters are given in Table II. For  $^{17}\text{C}$  two initial binding energies are considered. The first is the known neutron separation energy, the other takes into account the extra binding due to the first excited state at  $E^* = 1.77$  MeV. Previous experimental and theoretical information on  $^{17}\text{C}$  can be found in [48]. In the case of  $^{19}\text{C}$  we consider four possible initial binding energies:  $\varepsilon_i = -0.24$  MeV and  $-0.5$  MeV are two possible neutron binding energies close to the values from mass evaluation [49,50] and breakup experiments [7,8] discussed in the literature;  $-1.86$  MeV and  $-2.12$  MeV are the corresponding binding energies of a single particle state coupled to the  $2^+$  excited state of  $^{18}\text{C}$  which has  $E^* = 1.62$  MeV.

The optical potentials used to calculate the neutron-target  $S$ -matrix are the same used in [15], namely Refs. [51,52] for  $^9\text{Be}$ ,  $^{12}\text{C}$ , and  $^{208}\text{Pb}$ , respectively. For each fixed initial state the breakup cross section absolute values are sensitive to both the neutron target optical potential and to the core survival probability. This effect has been carefully analyzed in a series of publications [15,25,33,40] and it is at present being

TABLE III.  $^{19}\text{C}$  results at  $E_{inc} = 88\text{A}$  MeV with sharp cutoff.

$ \varepsilon_i $ (MeV)	$\hbar\Delta k_1$ (MeV/c)			$\sigma_{1n}$ (mb)		
0.24	28	109	100	441	87	72
0.50	37	130	120	270	63	55
1.86	65	171	160	94	32	29
Initial state	$2s_{1/2}$	$1d_{5/2}$	$1d_{3/2}$	$2s_{1/2}$	$1d_{5/2}$	$1d_{3/2}$

studied by several authors, including us. In particular, as has been suggested in [25,40], it is possible that it will be necessary to modify the parametrization of the presently available  $n$ - $^9\text{Be}$  optical potentials which were fitted mainly on low or very high energy free particle cross sections. We estimate that this modification could reduce the cross sections on  $^9\text{Be}$  up to about 30% of the values shown here, still leaving them within the experimental uncertainty. On the other hand the results discussed for the other targets should be unaffected since the calculated free neutron cross sections agree well with the known experimental data.

The cross section values and momentum distribution widths for the reaction of  $^{19}\text{C}$  on  $^9\text{Be}$  at  $E_{inc} = 88\text{A}$  MeV are shown in Table III where the sharp cutoff approximation to Eq. (2.3) was used with  $R_s = 1.4(A_p^{1/3} + A_T^{1/3})$  fm. In Table IV we give the values obtained by the smooth cutoff approximation Eq. (2.4) with  $a = 0.6$  fm. All values in the tables are obtained by setting the initial state spectroscopic factor  $C^2S$  equal to one. Separate contributions from elastic breakup and absorption are also given. Our sample calculations have shown a smooth variation of the breakup cross sections with  $a$ , a further increase of its value up to 0.7 fm gives a negligible increase in the cross sections of about 1%. Therefore the variation in the values of Tables III and IV gives an estimate of the possible uncertainty in the treatment of the core-target interaction. It appears that an increase of 50% in the absolute value of the initial binding gives a decrease in the breakup cross section of 50–60% while the widths increase by less than 30%. The differences between the results in the case of an initial  $d_{5/2}$  or  $d_{3/2}$ , both taken at the same binding energy, are instead of the order of 10%. The effect of the smooth cutoff is negligible in the case of an  $s$  state with very small binding. This is because the free-particle limit to halo breakup discussed in [15,26] applies in

TABLE IV.  $^{19}\text{C}$  results at  $E_{inc} = 88\text{A}$  MeV with smooth cutoff and  $C^2S = 1$ . Using  $0.6 \times (0^+ \otimes 2s_{1/2}) + 0.4 \times (2^+ \otimes d_{5/2})^{(2)}$ , we get  $\sigma_{1n} = 200$  mb and  $\hbar\Delta k_1 = 40$  MeV/c, while  $\sigma_{1n} = 150 \pm 40$  mb [53],  $\Gamma_{exp} = 42 \pm 4$  MeV/c [7].

$ \varepsilon_i $ (MeV)	$\hbar\Delta k_1$ (MeV/c)			$(\sigma_{el} \ \sigma_{abs})$	$\sigma_{1n}$	
				(mb)	(mb)	
<sup>(1)</sup> 0.24	29	141	132	(194 248)442	(42 63)105	(34 53)87
<sup>(2)</sup> 0.50	41	157	148	(129 173)302	(31 50) 81	(27 45)72
<sup>(1)</sup> 1.86	68	197	177	(53 83)136	(18 33) 51	(15 29)44
<sup>(2)</sup> 2.12	—	216	—	—	(16 31) 47	—
Initial state	$2s_{1/2}$	$1d_{5/2}$	$1d_{3/2}$	$2s_{1/2}$	$1d_{5/2}$	$1d_{3/2}$

TABLE V.  $^{17}\text{C}$  results at  $E_{inc}=84\text{A}$  MeV with smooth cutoff and  $\text{C}^2\text{S}=1$ . Using  $0.16 \times (2^+ \otimes 2s_{1/2}) + 1.58 \times (2^+ \otimes d_{5/2})$  we get  $\sigma_{1n}=96$  mb and  $\hbar\Delta k_1=142$  MeV/c, while  $\sigma_{1n}=60 \pm 20$  mb [53] and  $\Gamma_{exp}=145 \pm 5$  MeV/c [7],  $\sigma_{1n}=129 \pm 22$  mb [54],  $\Gamma_{exp}=141 \pm 6$  MeV/c [9,54].

$ \varepsilon_i $ (MeV)	$\hbar\Delta k_1$ (MeV/c)			$\sigma_{1n}$ (mb)		
0.73	45	152	142	238	65	58
2.50	71	191	171	127	48	40
Initial state	$2s_{1/2}$	$1d_{5/2}$	$1d_{3/2}$	$2s_{1/2}$	$1d_{5/2}$	$1d_{3/2}$

this case. In the other cases one sees that the importance of the smooth cutoff increases with the binding energy. To give an idea of the sensitivity of the breakup cross section on the strong absorption radius we have varied  $R_s$  to the values  $R_s=7$  fm, 7.5 fm, 8 fm, and 8.5 fm obtaining for the cross section the following values respectively  $\sigma_{1n}=270$  mb, 214 mb, 184 mb, 153 mb, for an initial  $s$ -state with binding  $-0.5$  MeV, and smooth cutoff with  $a=0.6$ .

To complete the discussion on  $^{19}\text{C}$  we have calculated the nuclear diffraction component of the breakup, due to the first term of Eq. (2.1), at  $E_{inc}=67\text{A}$  MeV for the  $^{12}\text{C}$  and  $^{208}\text{Pb}$  targets used in the exclusive RIKEN experiment [8]. The measured cross sections of [8] are  $82 \pm 14$  mb and  $1.34 \pm 0.12$  b, respectively. The value on the  $^{12}\text{C}$  target is supposed to be due only to the nuclear elastic breakup, while the value on the lead target is mainly due to Coulomb breakup. In [8] a spectroscopic factor of 0.67 is extracted for the  $0^+ \otimes 2s_{1/2}$ . Also the analysis in [12,39] of the measured interaction cross section suggests a rather large  $s$  component. In particular the authors of [12] found their experimental results consistent with a configuration having 46% ( $0^+ \otimes 2s_{1/2}$ ) and 54% ( $2^+ \otimes d_{5/2}$ ).

Using the option (2) for the separation energies of Table IV, which means 0.5 MeV for the  $s$  state and 2.12 MeV for the  $d$  state, we find a good agreement with the RIKEN experimental results if we assume a spectroscopic factor of 0.6 for the  $s$  state and of 0.4 for the  $d$  state and sum both contributions. Then we obtain  $\sigma_{el}=93$  mb on  $^{12}\text{C}$  and  $\sigma_{el}=273$  mb on the lead target. Our estimate for the Coulomb breakup of the  $s$  state on lead is  $\sigma_{Coul}=1125$  mb, such that in the latter case our total exclusive breakup cross section is  $\sigma_{tot}=1398$  mb. Following the prescription [14,15,37]  $R_s=1.4(A_P^{1/3}+A_T^{1/3})$  fm, we took  $R_s=6.9$  fm for the  $^{12}\text{C}$  target and  $R_s=12$  fm for the  $^{208}\text{Pb}$  target. It is interesting to notice that we extract the same spectroscopic factor from the light and heavy target data, thus showing that our model and the choice of parameters used, such as  $R_s$ , are appropriate for the description of the nuclear part of the breakup cross section both on a light as well as a heavy target.

With the same spectroscopic factors and combination of  $s$  and  $d$  states, the results at 88A MeV are given at the top of Table IV. The cross section value is in good agreement with the recent measurements from MSU  $\sigma_{1n}=150 \pm 40$  mb [53] and it is consistently smaller than that from the relativistic energy GSI experiment  $\sigma_{1n}=233 \pm 51$  mb [54]. Our width is in good agreement with the MSU value  $\Gamma_{exp}=42 \pm 4$  MeV/c [7] but, as expected it is smaller than the GSI

spectrum width  $\Gamma_{exp}=69 \pm 3$  MeV/c [9]. Actually we find the best agreement with the shape of the tails of the spectrum from [7] if we take 30% of  $s$  state and 70% of  $d$  state, in option (2) for the separation energies of Table III. Clearly because of the present uncertainty on the neutron separation energy of  $^{19}\text{C}$  we conclude that the  $s$  state can be present with 30–60% occupation in the  $^{19}\text{C}$  ground state.

In [9] it has been suggested that possible discrepancies in the measured widths from different laboratories could originate from an incident energy dependence of the reaction mechanism. We have discussed in detail such a dynamical effect in [15,16] and in the first part of this paper. It is however puzzling that the discrepancy in the measured widths from  $^{19}\text{C}$  breakup does not seem to be present in the case of  $^{17}\text{C}$  discussed in the following. A possible explanation has recently been proposed in [55].

The results for  $^{17}\text{C}$  breakup at  $E_{inc}=84\text{A}$  MeV are shown in Table V. The values in the table are again obtained with unity spectroscopic factors and smooth cutoff. At the top of Table V are reported the values for the cross sections and the widths of the parallel momentum distribution obtained summing the  $s$  and  $d$  contributions, both coupled to the core  $2^+$  state, which means initial separation energy of 2.50 MeV, using instead the spectroscopic factors quoted in [7], namely  $0.16 \times (2^+ \otimes 2s_{1/2}) + 1.58 \times (2^+ \otimes d_{5/2})$ . Some experimental values from [7,54,53] are also given. Our results are consistent with both experiments. From the results given in the table we see that the breakup from an initial pure  $1d_{3/2} \otimes 0^+$  state, with binding  $-0.73$  MeV, and the breakup from the state  $0.16 \times (2^+ \otimes 2s_{1/2}) + 1.58 \times (2^+ \otimes d_{5/2})$  both give reasonable agreement with the widths of the present data although the shape of the experimental spectrum [7,9] seems to agree better with the calculation of the latter case, when the core is excited. Our cross section  $\sigma_{1n}=93$  mb is in good agreement with the recent result from MSU  $\sigma_{1n}=60 \pm 20$  mb [53] which was obtained in an exclusive  $\gamma$ -ray experiment in which the core breakup from the  $2^+$  state was identified. On the other hand it seems possible that adding to the calculated cross section for the  $0.16 \times (2^+ \otimes 2s_{1/2}) + 1.58 \times (2^+ \otimes d_{5/2})$  configuration a contribution of about 50% from the  $1d_{3/2} \otimes 0^+$ , a better agreement with the experimental inclusive [9] cross section value could be obtained.

## V. CONCLUSIONS

In this paper we have applied the transfer to the continuum theory in the formulation which includes spin to the

study of the breakup of two weakly bound carbon isotopes for which the  $d$  orbital is important. The present theory can be viewed as a generalization of sudden eikonal theories which are obtained from our formalism taking the limit of zero initial neutron binding energy. The utility of a time-dependent approach with spin coupling in the treatment of breakup from  $d$  orbitals of not too weak binding has been clarified.

Some hypotheses on the occupancy of the  $s$ - $d$  shells in  $^{19}\text{C}$  and  $^{17}\text{C}$  have been formulated by comparing some of the existing experimental data with our theoretical calculations. Our conclusion is that in  $^{19}\text{C}$  the breakup neutron occupies the  $d$  state with 40–70 % probability while the  $s$  state has a 30–60 % occupation probability. The present uncertainty on the neutron separation energy does not allow any definite conclusion. The  $s$  state is coupled to the ground state when we get the best agreement with the data, therefore the total  $^{19}\text{C}$  spin should be  $1/2^+$ . The extreme characteristics of the  $s$  state are responsible for the large neutron breakup cross section and narrow ejectile parallel momentum distribution.

For  $^{17}\text{C}$ , on the basis of the available experimental spectra, the breakup from the  $(1d_{3/2} \otimes 0^+)$  configuration seems to show up less than the breakup of the  $s$ - $d$  states coupled to the core  $2^+$ . In the two cases where the resulting spectra have similar widths, however, due to the spin coupling effects, the

spectrum of the  $d_{3/2}$  breakup should show a characteristic asymmetry which does not seem to correspond to the MSU data nor to the GSI spectrum. New data from MSU [53] will soon be available which hopefully will help clarify the situation.

Our model takes into account the fact that breakup reactions are sensitive only to the outermost tails of the single particle initial state wave functions which we take as Hankel functions. It would be very important to check with more refined structure calculations whether our hypothesis on the occupation of the  $s$  and  $d$  states are correct. It would also be very useful to make other experiments, like the  $\gamma$ -rays ones of [47,53] in which breakup from initial core excited states can be measured. Finally we have suggested that a study of the neutron transverse distribution from the experimental point of view, as already done in [41], could help resolve some puzzling cases with the help of spin dependent reaction models like the one discussed here which contains also interference effects between the parallel and transverse momentum distributions.

#### ACKNOWLEDGMENTS

I wish to thank P. G. Hansen and A. Mengoni for communicating their recent results.

- 
- [1] I. Tanihata *et al.*, Phys. Lett. **160B**, 380 (1985).  
 [2] P. G. Hansen, A. S. Jensen, and B. Jonson, Annu. Rev. Nucl. Part. Sci. **45**, 591 (1995).  
 [3] W. Schwab *et al.*, Z. Phys. A **350**, 238 (1995).  
 [4] I. Pecina *et al.*, Phys. Rev. C **52**, 191 (1995).  
 [5] F. Negoita *et al.*, Phys. Rev. C **54**, 1787 (1996).  
 [6] D. Bazin *et al.*, Phys. Rev. Lett. **74**, 3569 (1995).  
 [7] D. Bazin *et al.*, Phys. Rev. C **57**, 2156 (1998).  
 [8] T. Nakamura *et al.*, in *ENAM98: Exotic Nuclei and Atomic Masses*, 1998, edited by Bradley M. Sherrill, David J. Morrissey, and Cary N. Davids, AIP Conf. Proc. No. 455 (AIP, New York, 1998); A. Mengoni, Report No. nucl-th/9812065, to appear in the Proceedings of the VII Congresso di Fisica Nucleare Teorica, Cortona, Italy.  
 [9] T. Baumann *et al.*, Phys. Lett. B **439**, 256 (1998).  
 [10] F. M. Marques *et al.*, Phys. Lett. B **381**, 407 (1996).  
 [11] M. G. Saint-Laurent *et al.*, Z. Phys. A **332**, 457 (1989).  
 [12] A. Ozawa *et al.*, Report No. RIKEN-AF-NP-294, 1998, submitted to Phys. Rev. Lett.  
 [13] A. Bonaccorso, Nucl. Phys. **A649**, 315c (1999).  
 [14] A. Bonaccorso and D. M. Brink, Phys. Rev. C **57**, R22 (1998).  
 [15] A. Bonaccorso and D. M. Brink, Phys. Rev. C **58**, 2864 (1998).  
 [16] A. Bonaccorso and D. M. Brink, Phys. Rev. C **38**, 1776 (1988).  
 [17] A. Bonaccorso and D. M. Brink, Phys. Rev. C **43**, 299 (1991).  
 [18] A. Bonaccorso and D. M. Brink, Phys. Rev. C **44**, 1559 (1991).  
 [19] A. Bonaccorso and D. M. Brink, Phys. Rev. C **46**, 700 (1992).  
 [20] A. Bonaccorso, I. Lhenry, and T. Suomijarvi, Phys. Rev. C **49**, 329 (1994).  
 [21] R. Anne *et al.*, Nucl. Phys. **A575**, 125 (1994).  
 [22] J. K. Kelley *et al.*, Phys. Rev. Lett. **74**, 30 (1995).  
 [23] G. Baur, F. Rosel, D. Trautmann, and R. Shyam, Phys. Rep. **111**, 333 (1984).  
 [24] R. Shyam and H. Lenske, Phys. Rev. C **57**, 2427 (1998).  
 [25] K. Hencken, G. F. Bertsch, and H. Esbensen, Phys. Rev. C **54**, 3043 (1996); G. F. Bertsch, G. F. Bertsch, K. Hencken, and H. Esbensen, *ibid.* **57**, 1366 (1998).  
 [26] P. G. Hansen, Phys. Rev. Lett. **77**, 1016 (1996).  
 [27] C. A. Bertulani and K. W. McVoy, Phys. Rev. C **46**, 2638 (1992).  
 [28] Y. Ogawa, K. Yabana, and Y. Suzuki, Nucl. Phys. **A543**, 722 (1992); Y. Ogawa and I. Tanihata, *ibid.* **A616**, 239c (1997).  
 [29] F. Barranco, E. Vigezzi, and R. A. Broglia, Z. Phys. A **356**, 45 (1996).  
 [30] H. Sagawa and N. Takigawa, Phys. Rev. C **50**, 985 (1994).  
 [31] A. A. Korshennikov and T. Kobayashi, Nucl. Phys. **A576**, 97 (1994).  
 [32] H. Esbensen, Phys. Rev. C **53**, 2007 (1996).  
 [33] E. Garrido, D. V. Fedorov, and A. S. Jensen, Phys. Rev. C **59**, 1272 (1999).  
 [34] H. Esbensen and G. F. Bertsch, Phys. Rev. C **59**, 3240 (1999).  
 [35] L. Lo Monaco and D. M. Brink, J. Phys. G **11**, 935 (1985).  
 [36] H. Hashim and D. M. Brink, Nucl. Phys. **A476**, 107 (1988).  
 [37] A. Bonaccorso, D. M. Brink, and L. Lo Monaco, J. Phys. G **13**, 1407 (1987).  
 [38] J. A. Christley *et al.*, Nucl. Phys. **A6624**, 275 (1997).

- [39] J. A. Tostevin and J. S. Al-Khalili, Phys. Rev. C **59**, R5 (1999).
- [40] J. A. Tostevin, J. Phys. G **25**, 735 (1999).
- [41] L. V. Chulkov *et al.*, Phys. Rev. Lett. **79**, 201 (1997); L. V. Chulkov and G. Schrieder, Z. Phys. A **359**, 231 (1997).
- [42] W. Von Oertzen, Phys. Lett. **151B**, 95 (1985).
- [43] E. K. Barburton and B. A. Brown, Phys. Rev. C **46**, 923 (1992).
- [44] Ren Zhongzhou, Z. Y. Zhu, Y. H. Cay, and Xu Gongou, Nucl. Phys. **A605**, 75 (1996).
- [45] D. Ridikas, M. H. Smedberg, J. S. Vaagen, and M. V. Zhukov, Europhys. Lett. **37**, 385 (1997).
- [46] D. Ridikas, M. H. Smedberg, J. S. Vaagen, and M. V. Zhukov, Nucl. Phys. **A628**, 363 (1998).
- [47] A. Navin *et al.*, Phys. Rev. Lett. **81**, 5089 (1998).
- [48] J. A. Nolen *et al.*, Phys. Lett. **71B**, 316 (1997).
- [49] R. W. Finlay *et al.*, Phys. Rev. C **47**, 237 (1993).
- [50] N. A. Orr *et al.*, Phys. Lett. B **258**, 29 (1991), and references therein.
- [51] J. H. Dave and C. R. Gould, Phys. Rev. C **28**, 2212 (1983).
- [52] C. Mahaux and R. Sartor, Adv. Nucl. Phys. **20**, 1 (1991).
- [53] V. Maddalena *et al.*, private communication. Note: Experiment performed 60A MeV.
- [54] D. Cortina-Gil *et al.*, in XXXVII Winter Meeting in Nuclear Physics, Bormio, 1999, edited by I. Iori, Ricerca Scientifica ed Educazione Permanente, Supplemento n. 114, 1999, p. 428.
- [55] M. H. Smedberg and M. V. Zhukov, Phys. Rev. C **59**, 2048 (1999).